

# DEVELOPMENT OF FAST HELIUM BEAM EMISSION SPECTROSCOPY FOR PLASMA DENSITY- AND TEMPERATURE DIAGNOSTICS

M. Proschek, S. Menhart, H. D. Falter, H. Anderson<sup>a</sup>, H. P. Summers<sup>a</sup>, A. Stabler<sup>b</sup>, P. Franzen<sup>b</sup>, H. Meister<sup>b</sup>, J. Schweinzer<sup>d</sup>, T.T.C. Jones<sup>c</sup>, S. Cox<sup>c</sup>, N. Hawkes<sup>c</sup>, F. Aumayr, and HP. Winter

Institut f. Allgemeine Physik, TU-Wien, A-1040 Wien, Wiedner Hauptstrasse 8-10  
(Association EURATOM-OEAW)

<sup>a</sup>Dept. of Physics and Applied Physics, Univ. of Strathclyde, Glasgow, UK

<sup>b</sup>Max-Planck-Institut f. Plasmaphysik, D-85748 Garching

<sup>c</sup>UKAEA-Euratom Association, Culham Science Centre, Abingdon, OXON, OX14 3EA, UK

<sup>d</sup>EFDA-JET CSU, Building K1, Culham Science Centre, Abingdon, OXON, OX14 3EA, UK

E-mail: falter@iap.tuwien.ac.at

**Abstract.** For developing a novel electron density and -temperature diagnostics based on fast He beam emission spectroscopy, experiments have been performed at the ASDEX Upgrade tokamak (AUG) in Garching and the JET tokamak in Culham. The measured He I emission profiles were compared with model calculations which are based on a collisional-radiative model developed by the ADAS group. For exploratory measurements at AUG one of the heating beam sources has been operated with pure helium. The beam emission profiles show satisfactory agreement with the profiles modelled using density and temperature profiles from other diagnostics. At JET and recently at AUG a small amount of helium was added to one standard deuterium ion source in order to produce a “doped” helium/deuterium beam. The respective measurements were performed using groups of identical pulses. In total, 11 different He I lines were investigated at JET with respect to their dependence on plasma density and -temperature. Seven lines were found to have sufficient intensity but the beam emission profile suffers from limited bandwidth of the spectrometer used. Good beam emission profiles could be obtained from recent AUG measurements showing a scatter of 9%.

## 1. Introduction

Optical emission from energetic lithium beams [1] has been successfully used as a diagnostic of plasma density. Thermal helium beams [2] have been used to measure electron temperature and -density. Both diagnostics are limited in range to the outer regions of the plasma by the small penetration depth of the neutral particles. Energetic helium atoms penetrate much deeper into the plasma than either lithium atoms of similar energy or thermal helium atoms, and therefore offer the prospect of a localised measurement of electron temperature and plasma density over a wider range than accessible with either lithium - or thermal He beams. Of particular interest are measurements with a high spatial resolution extending over H mode - or internal transport barrier.

## 2. The Collisional-Radiative Model

The line emission of fast He atoms in a plasma has been modelled previously by several groups [3,4] by adding ion-impact excitation and -ionisation to the model used for thermal He beams. Recently a collisional-radiative (cr)-model for He beams (ADAS311, ADAS313) has been developed by the ADAS group at the University of Strathclyde, Glasgow [5], which takes into account electron- and ion impact excitation, de-excitation, ionisation, charge exchange between He and fully stripped ions, and spontaneous emission from excited He states.

The local population density  $N_i$  of atoms in state  $i$  of a He beam penetrating a plasma along the beam direction  $x$  can be determined by stepwise solving the balance equations, which can be written in matrix form:

$$v_b \frac{dN_i}{dx} = \sum_j C_{ij} N_j \quad (1)$$

$C_{ij}$  is called the collisional-radiative matrix, which includes all the collisional- and spontaneous emission contributions mentioned above,  $v_b$  is the beam velocity. The matrix elements  $C_{ij}$  are functions of the local electron- and ion temperature ( $T_e$ ,  $T_i$ ), electron- and ion density ( $n_e$ ,  $n_i$ ) and beam energy ( $E_b$ ). Excited states are treated as being in equilibrium with the ground state ( $1^1S$ ) and the two metastable states ( $2^1S$  and  $2^3S$ ). With the population profiles of the ground - and metastable states and the so-called “effective beam emission coefficients  $E_{ij}$ ” (EECs) generated by ADAS313 using the relation

$$E_{ij} = A_{ij} \frac{N_i(T_e, n_e, E_b, N_k)}{n_e N_k(T_e, n_e, E_b)} \quad (2)$$

the emission profile is calculated. More details of the model are given in [6].

### 3. Sensitivity Analysis

Based on temperature - and density profiles from a JET ITB discharge (#40554) the sensitivity of the visible HeI beam emission has been assessed by comparing the calculated beam emission of the steady profiles with that from profiles composed of steps and flat sections in either the temperature - or the density profile. Fig. 1 shows an example from the scrape off layer. The corresponding emission profiles are shown in Fig. 2 for a beam with an initial metastable  $2^3S$  fraction of 10%. Experimental evidence indicates that the intensity has to be above  $10^{16}$  to be detectable. This limit is marked as grey band in Fig. 2. To quantify the diagnostic relevance of the line emission we use the ratios  $S_n$  and  $S_T$  defined as

$$S_n = \frac{\Delta I/I}{\Delta n/n} \quad S_T = \frac{\Delta I/I}{\Delta T/T}$$

$S_n$  and  $S_T$  denote the normalised change in intensity  $\Delta I/I$  related to the normalised step in intensity  $\Delta n/n$  or temperature  $\Delta T/T$ , respectively.

#### 3.1 Scrape-off layer

All singlet lines are quite sensitive to changes in density with values for  $S_n$  between 1.13 and 0.33. The  $2^1P-3^1D$  transition (668 nm) shows a good and almost constant sensitivity over the full range, and at the same time a low sensitivity to temperature variations.  $S_T$ , the sensitivity against temperature, is large at the edge and reduces significantly towards the core.

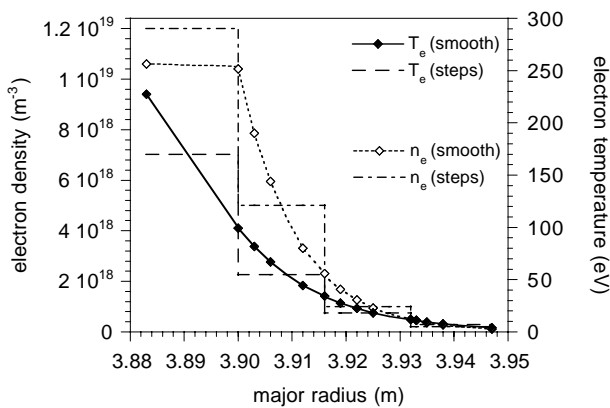


FIG. 1: Profiles used for the sensitivity analysis in the plasma edge region.

The sensitivity against density is higher than that against temperature. Near the separatrix ( $R=3.901$ ) most triplet lines show a considerably reduced temperature sensitivity. In order to derive temperature- and density profiles one would ideally look for transitions which are mainly sensitive to only one of the two parameters. For the density profile the  $2^1S-3^1D$  transition at 668 nm appears to be most suitable, showing high sensitivity against density and a low one against temperature. None of the transitions has a low sensitivity to density and a high sensitivity to temperature, but

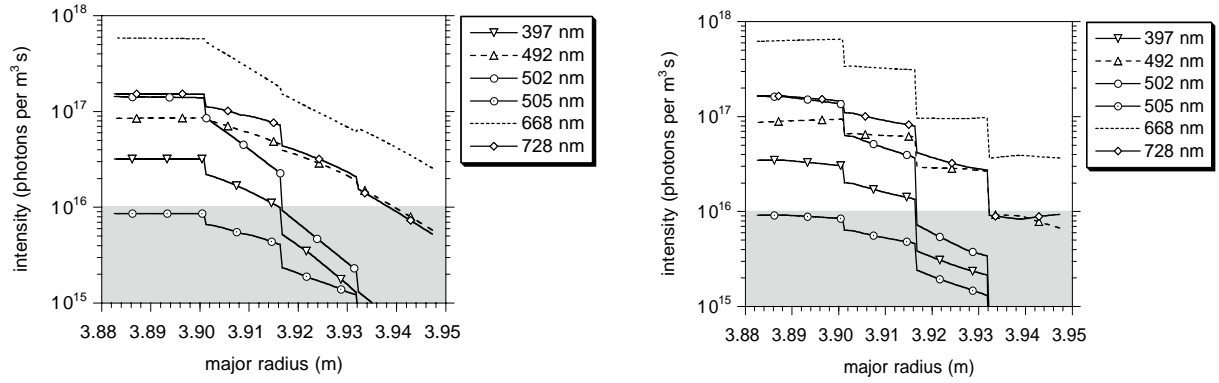


FIG. 2: Beam emission profiles in the plasma edge region. The shaded area marks the sensitivity limit of the JET KS7.

Left: Emission profile with smooth density profile and temperature profile with steps. Right: Emission profile with smooth temperature profile and density profile with steps.

there are some transitions with a reasonable sensitivity to temperature, namely  $2^3\text{S}-3^3\text{P}$  (389 nm), and all the singlet transitions apart from  $2^1\text{P}-4^1\text{D}$  (492 nm) and  $2^1\text{P}-3^1\text{D}$  (668 nm).

### 3.2 Core region

We use again the profiles from the JET ITB discharge 40554, before and after ITB formation. The profiles are then sectioned as shown in Fig. 3. Plasma temperature and - density are rather high and the beam attenuation of the initial ground state population in the plasma centre is 72% before ITB formation and 64% after ITB formation. The sensitivity analysis is identical to the procedure used for the scrape off layer and the results are summarised in table I.

|               | major     | Te        | Ne                       | $S_n$  |             |             |             |             |        |  |
|---------------|-----------|-----------|--------------------------|--------|-------------|-------------|-------------|-------------|--------|--|
|               | radius    | keV       | $10^{19} \text{ m}^{-3}$ | 397 nm | 492 nm      | 502 nm      | 505 nm      | 668 nm      | 728 nm |  |
| Singlet lines | 3.6       | 2.15      | 1.1-1.48                 | 0.49   | <b>0.56</b> | <b>0.81</b> | 0.43        | <b>0.78</b> | 0.42   |  |
|               |           | 2.4       | 1.25-2.00                | 0.43   | <b>0.53</b> | <b>0.81</b> | 0.35        | <b>0.78</b> | 0.33   |  |
|               | 3.35      | 4.5       | 1.48-2.1                 | 0.39   | <b>0.5</b>  | <b>0.78</b> | 0.29        | <b>0.76</b> | 0.27   |  |
|               |           | 3.7       | 2.00-3.15                | 0.26   | 0.42        | <b>0.77</b> | 0.12        | <b>0.75</b> | 0.09   |  |
|               | 3.12      | 7.5       | 2.1-2.55                 | 0.27   | 0.44        | <b>0.78</b> | 0.14        | <b>0.76</b> | 0.10   |  |
|               |           | 9.0       | 3.15-4.1                 | 0.36   | 0.49        | <b>0.64</b> | 0.34        | <b>0.67</b> | 0.33   |  |
|               |           |           |                          |        | $S_T$       |             |             |             |        |  |
|               | 3.6       | 1.00-3.35 | 1.20                     | -0.09  | -0.26       | -0.14       | -0.11       | -0.25       | 0.14   |  |
|               | 3.35      | 3.35-6.00 | 1.75                     | -0.07  | -0.21       | -0.12       | 0.00        | -0.17       | 0.23   |  |
| 3.12          | 6.00-7.70 | 2.46      | 0.03                     | -0.06  | -0.01       | 0.08        | -0.02       | 0.21        |        |  |
| Triplet lines | major     | Te        | Ne                       | $S_n$  |             |             |             |             |        |  |
|               | radius    | keV       | $10^{19} \text{ m}^{-3}$ | 389 nm | 447 nm      | 471 nm      | 588 nm      | 707 nm      |        |  |
|               | 3.6       | 2.15      | 1.1-1.48                 | 0.30   | 0.38        | 0.33        | <b>0.51</b> | 0.36        |        |  |
|               |           | 2.4       | 1.25-2.00                | 0.22   | 0.33        | 0.26        | <b>0.51</b> | 0.31        |        |  |
|               | 3.35      | 4.5       | 1.48-2.1                 | 0.15   | 0.25        | 0.17        | 0.46        | 0.23        |        |  |
|               |           | 3.7       | 2.00-3.15                | -0.14  | 0.06        | -0.07       | 0.35        | 0.02        |        |  |
|               | 3.12      | 7.5       | 2.1-2.55                 | -0.13  | 0.04        | -0.09       | 0.35        | 0.01        |        |  |
|               |           | 9.0       | 3.15-4.1                 | 0.17   | 0.22        | 0.19        | 0.30        | 0.21        |        |  |
|               |           |           |                          |        | $S_T$       |             |             |             |        |  |
|               | 3.6       | 1.00-3.35 | 1.20                     | 0.17   | 0.01        | 0.00        | -0.24       | -0.14       |        |  |
| 3.35          | 3.35-6.00 | 1.75      | 0.2                      | 0.11   | 0.08        | -0.2        | -0.11       |             |        |  |
| 3.12          | 6.00-7.70 | 2.46      | 0.12                     | 0.10   | 0.07        | -0.16       | -0.11       |             |        |  |

TAB. I: SENSITIVITY IN THE CORE REGION of a JET ITB discharge before (black) and after (blue) ITB formation. 10% initial metastable  $2^3\text{S}$  fraction.

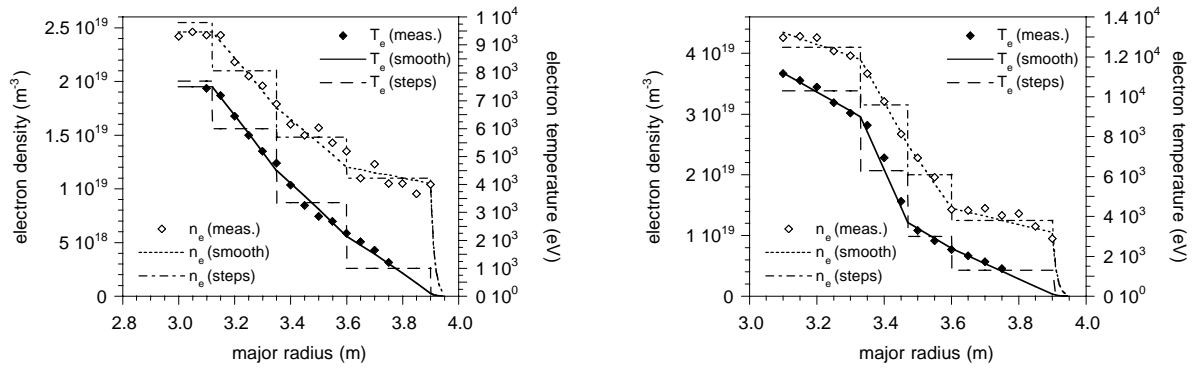


FIG. 3: Temperature and density profiles used for the sensitivity analysis in the plasma core. Left: before ITB formation, right: after ITB formation.

The singlet transitions  $2^1S-3^1P$  (502 nm) and  $2^1P-3^1D$  (668 nm) have a high and almost constant sensitivity to density and very little variation before and after ITB formation. These two lines also show a small sensitivity to temperature and appear well suited for deriving the density profile. Again, as in the edge region, none of the lines is mainly sensitive to temperature. The best candidates for temperature profiles are the transitions  $2^1P-3^1S$  (728 nm) and  $2^3S-3^3P$  (389 nm). As a starting point for profile evaluation we will probably attempt to derive the density profile from line  $2^1P-3^1D$  (668 nm), which also happens to be the most intense one. The temperature profile will then be derived from either the  $2^1P-3^1S$  (728 nm) or the  $2^3S-3^3P$  (389 nm) transitions making use of the already known density profile.

## 4 Experiments

Experiments with He beam emission have been carried out at the AUG and JET tokamaks. The first experimental campaign at AUG used a pure 30 keV Helium beam from one beam source of the SO injector. This required to modify one beam source from deuterium operation to helium. The respective beam source was therefore not available for plasma heating and He injection was restricted to a 300 ms pulse at the end of the injection sequence. Later experiments at JET and AUG made use of a doped deuterium/helium beam [7]. The doped beam enables He beam emission experiments without reducing the availability of the neutral beam heating system. In both experiments a spectrometer normally used for ion temperature measurements could be utilized for measuring the He beam emission of interest.

### 4.1 Results

For our first measurements at the AUG tokamak (IPP Garching) we have used a 30 keV Helium beam in position 4 of the so-called SO injector and the CER spectrometer with 16 lines of sight. By only using the Doppler shifted helium line, the intensity of the beam emission could be separated from the background. For the outer lines of sight the viewing angle was too close to  $90^\circ$  and the Doppler shifted beam emission was masked by the HeI background emission, which was more intense by one order of magnitude. The intensity of the triplet line (Fig. 4 left) is dominated by the attenuation of the metastable triplet fraction and shows a rapid decrease in signal level towards the plasma centre. The singlet line (Fig. 4 right) is visible over the entire range from edge to plasma centre. In both cases we observe a satisfactory agreement between measured and modelled beam emission profiles. Beam emission profiles could be measured for the transitions  $2^1P-3^1D$ ,  $2^1S-3^1P$ , and  $2^3P-3^3D$ . Other lines were also investigated but showed insufficient intensity. From more recent measurements on AUG using beam source 3 we will be able to compare a wider range of the beam emission profile as we have a more favourable viewing angle onto the beam of PINI 3. From these measurements we can also estimate the error of the measurements. Using the data from 3 identical discharges we obtain a scatter in the beam emission data of  $\pm 9\%$ .

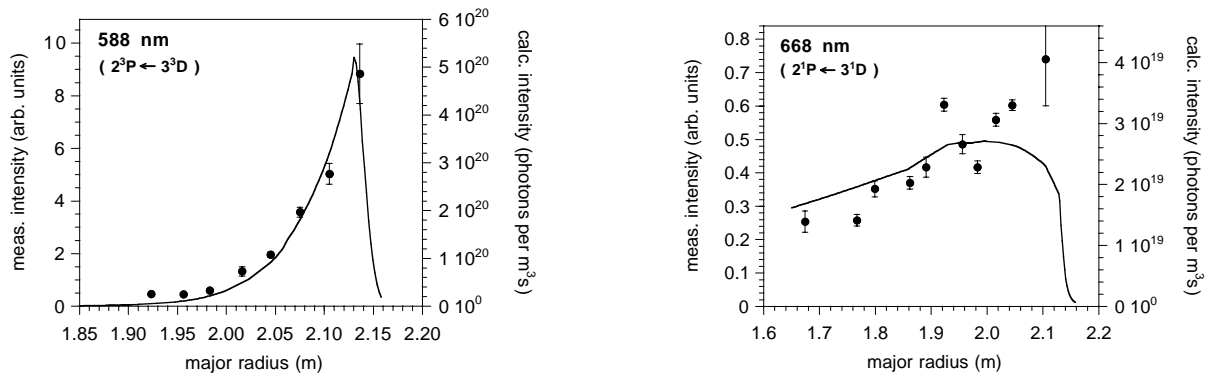


Fig. 4: Comparison of measured (solid circles) and modelled (lines) beam emission profiles from two AUG discharges.

The experimental data are from so called standard H mode pulses taken at 3.5 - 4 s. Due to the more favourable viewing angle these recent experiments also yielded beam emission profiles extending right to the plasma edge. These profiles will be compared with extended modelling calculations treating all levels up to  $n=5$  as non equilibrium levels.

Experiments at JET showed that out of the 11 HeI lines in the visible range we could measure 7 with sufficient intensity for beam emission spectroscopy. The best signal to noise ratio was 150 with a time resolution of 50 ms. These beam emission profiles however suffered from too narrow a bandwidth of the spectrometer used and require large intensity corrections causing additional scatter. Further experiments avoiding this limitation are currently in preparation.

## 5. Conclusion and Outlook

Beam emission from fast He atoms offers the prospect for locally resolved plasma density diagnostics. There is potential to also derive the temperature profile from the beam emission profile, in particular in the edge region. So far, experimental results suffered from an insufficient bandwidth of the spectrometer used (JET) or from limits in the sensitivity (AUG). In the case of JET, the bandwidth could be improved by reducing the number of lines of sight from 16 to 6. The code for modelling the beam emission is being modified at the moment. In future all excited states up to  $n = 5$  will be regarded as non equilibrium states. Additionally the input of temperature and density profile will be streamlined making the code faster and more suited for deriving density- and temperature profiles from the beam emission profile.

## References

- /1/ E. Wolfrum, F. Aumayr, E. Hintz, D. Rusbült, R. P. Schorn, D. Wutte, and HP. Winter, Fast lithium – beam spectroscopy of tokamak edge plasmas, Rev. Sci. Instrum. 64, pp 2285-92 (1993)
- /2/ B. Schweer, M. Brix, and M. Lehnen, Measurement of edge parameters in TEXTOR-94 at the low and high field side with atomic beams, J. Nucl. Mater. 266-269, pp 673-8 (1999).
- /3/ M. Brix, Messung von Elektronentemperatur und -dichte mittels Heliumstrahldiagnostik im Randschichtplasma eines Tokamaks, PhD thesis, Ruhr-University Bochum (1998, unpublished)
- /4/ S. Sasaki et al, Rev. Sci. Instrum. 67 (1996) 3521-3529
- /5/ H. P. Summers, Atomic Data and Analysis Structure, User Manual, Internal Report, JET-IR(94) 06, JET Joint Undertaking, UK (1994)
- /6/ S. Menhart et al, Explorative studies for the Development of fast He beam plasma diagnostics, accepted for publication in the proceedings of 14<sup>th</sup> Intern. Conf. On Plasma Surface Interactions in Controlled Fusion devices (PSI) held in Rosenheim (Germany) 22. – 26 May 2000.
- /7/ H. D. Falter et al, Helium doped hydrogen or deuterium beam as cost effective and simple tool for plasma spectroscopy, accepted for publication in Rev. Sci. Instr. 71, October 2000.